Combust. Sci. Technol., 185: 435–453, 2013

ISSN: 0010-2202 print/1563-521X online
DOI: 10.1080/00102202.2012.726666

Taylor & Francis
Taylor & Francis Group

THE ROLE OF MOISTURE ON COMBUSTION OF PYROLYSIS GASES IN WILDLAND FIRES

Selina C. Ferguson,[1] Ambarish Dahale,[1] Babak Shotorban,[1] Shankar Mahalingam,[1] and David R. Weise[2]

[1]*Department of Mechanical and Aerospace Engineering, The University of Alabama in Huntsville, Huntsville, Alabama, USA*

[2]*Pacific Southwest Research Station, USDA Forest Service, Riverside, California, USA*

The role of water vapor, originated from the moisture content in vegetation, on the combustion process was investigated via simulating an opposed diffusion flame and a laminar premixed flame with pyrolysis gases as the fuel and air as the oxidizer. The fuel was mixed with water vapor, and the simulation was repeated for various water mole fractions. In both of the diffusion and premixed flames, the smaller the water mole fraction, the higher the maximum temperature. No reactions occurred when the water mole fraction was 0.65 or larger in the diffusion flame, and 0.70 or larger in the premixed flame. The maximum energy release rate and the flame speed decreased with the increase of the water mole fraction in the premixed flame. In both flames, O_2 and H were the components that showed dramatic changes with the change of the water mole fraction.

Keywords: Pyrolysis; Wildland fire

INTRODUCTION

Wildland fires can threaten life, property, and natural resources, or they can perform necessary ecological functions in many North American ecosystems. Therefore, it is important to develop combustion models to predict the behavior of wildfires, especially under rapid transition events, including marginal burning and transition to crown fires. A significant number of large fires in the United States occur in live fuels that contain significant moisture, and thus the influence of moisture content on fire behavior is significant.

One of the integral parts of wildland fires is the flame, which is sustained by gases that are released during pyrolysis of cellulose and hemicelluloses (Albini, 1981). A number of studies have been performed that focus on the modeling of fires using full, skeletal, or reduced mechanisms for combustion of pyrolysis fuel gases

Received 27 April 2012; revised 5 July 2012; accepted 30 August 2012.

Address correspondence to Babak Shotorban, Department of Mechanical and Aerospace Engineering, The University of Alabama in Huntsville, 5000 Technology Drive, Huntsville, AL 35899, USA. E-mail: babak.shotorban@uah.edu

(Lee et al., 2007; Leroy et al., 2008; Zhou and Mahalingam, 2001); however, the influence of moisture on the gaseous mixture that results from pyrolysis and its effect on flame structure have not been quantitatively studied. Moist fuel affects the rate and direction in which wildland fires spread. Moisture content is believed to slow the burning rate, since energy released from the flame first evaporates some moisture from the fuel particle before ignition occurs (Anderson, 1969). Tihay and Gillard (2010) investigate three Mediterranean species and conclude that H_2O, CO_2, CO, CH_4, and H_2 are the main gases released during pyrolysis of wood.

Previous studies (Fletcher et al., 2007; Morvan and Dupuy, 2004; Van Wagner, 1976; Zhou et al., 2005a, 2005b) have dealt with the effects of moisture in live vegetation during combustion, but there is no current study that specifically deals with the gaseous combustion fueled from pyrolysis of wood by investigating the role of moisture on the detailed flame structure. Manzello et al. (2007) studied the influence of moisture content on dead Douglas-fir trees in a laboratory experiment and showed that high moisture content (above 70% based on dry mass) inhibits the ability of the fire to initiate or sustain a flame. Furthermore, they showed that firebrand generation did not occur if the foliar and small branch moisture content was over 30% (dry mass basis). The studies of Bryden et al. (2002) and Bryden and Hagge (2003) indicate that moisture content affects the pyrolysis time of a biomass particle. They show that higher moisture content increases the pyrolysis time in a thermally thick and thermal wave regime. Beringer et al. (2003) investigated how fires in the tropical savanna in northern Australia were impacted by surface heat, moisture, and carbon fluxes. The frequency of fires in the tropical savanna was affected by the moisture content with the frequency of the fire occurrence increasing during dry seasons. Also in the study by Beringer et al. (2003), the intensity of the fire was affected by the moisture content. Drier seasons with lower moisture content resulted in fires with higher intensity. Likewise, seasons with high moisture contents resulted in fires with lower intensities. The intensity of the fires was estimated based on char and scorch heights using the relationship given by Williams et al. (1998). Fires that occurred in areas with high moisture content were found to have less char and lower scorch heights than areas that had lower moisture content.

The main purpose of the current research is to determine how moisture in the gaseous fuel caused by pyrolysis affects the behavior and characteristics of the flame in order to eventually determine a more accurate chemical mechanism for wildland fires involving live vegetation. An accurate chemical mechanism may allow improved prediction of wildland fires. The focus of this article is on understanding the role of varying fuel moisture mole fraction on pyrolysis gas flame structure. Toward this end, opposed diffusion and laminar premixed flames involving pyrolysis gases have been investigated. Several mechanisms have been previously studied for a chemical mechanism of gas emission from pyrolysis of wood such as GRI mechanism 3.0 (McDonald et al., 2000; Smith et al., 2000; Som et al., 2008). Since a detailed mechanism includes over 100 mechanisms and around 50 species, it is important to develop a reduced mechanism. In order to demonstrate that H_2O should be considered in the reduced mechanism, this study uses a skeletal mechanism reported by Zhou and Mahalingam (2001), which was created based on an updated mechanism included in GRI-Mechanism 3.0 (Smith et al., 2000).

DESCRIPTIVE SETUP OF SIMULATIONS

Opposed Diffusion Flame

An opposed diffusion flame (Lutz et al., 1997), a one-dimensional configuration with a planar diffusion flame between two opposed nozzles, is simulated with the OPPDIF software available in the CHEMKIN-Pro[1] software package (CHEMKIN-Pro, 2008). The program is based on a similarity transformation to reduce the three-dimensional flow field to a one-dimensional problem, making it more amenable for a detailed study. The opposed-flow geometry makes an attractive experimental configuration as well because the flames are flat, allowing for detailed study of the flame chemistry and structure.

In the opposed diffusion flame model considered in the present study, the pyrolytic fuel mixture enters from the left nozzle (boundary) located at $x = 0$ cm while the oxidizer enters from the right boundary at $x = 1$ cm. All simulations were carried out at standard temperature and pressure conditions. Both fuel and oxidizer stream velocities were set to 50 cm/s in simulations unless it is stated otherwise. In all cases, the oxidizer stream consisted of standard ambient air. A skeletal reaction mechanism was used in the current study with reactions tabulated in Table 1 (Zhou and Mahalingam, 2001). Parameters given in this table were used in the Arrhenius equation, which describes the relationship between the rate constant k of a chemical reaction, the activation energy E_a of the reaction and absolute temperature T:

$$k = AT^B \exp\left(-\frac{E_a}{RT}\right) \tag{1}$$

where R is the universal gas constant, A is the pre-exponential factor or A-factor, and B is the temperature exponent (CHEMKIN-Pro, 2008). In Table 1, the values of A and B were taken from the most recently updated reaction library of CHEMKIN-Pro.

In addition to four main pyrolysis gases of H_2, CH_4, CO_2, and CO considered by Zhou and Mahalingam (2001), H_2O in its gaseous phase was considered as an initial component to investigate the moisture effect. The simulations were conducted for three different woods: aspen (*Populus tremuloides*, type A), beech (*Fagus americana*, type B), and larch (*Larix sp.*, type C). These fuel types were modeled as mixtures of four gases with their mole fractions tabulated in Table 2 (Klose et al., 2000). In this table, the fuel gas mixture is assumed dry, i.e., $X_{H_2O} = 0$. To include the moisture effect, we scale the dry fuel species mole fractions tabulated in Table 2 according to the considered value of X_{H_2O}. Since the mole fraction of the fuel stream sums to 1.0, for instance, when 10% of H_2O gas is added to the fuel, the mole fractions of the fuel species are multiplied by 0.9 in order to account for the addition of H_2O. The mole fraction of H_2O was varied from 0 to 1.0. It is noted that the moisture content of living vegetation ranges from approximately 50% to over 300% (dry mass basis). chaparral vegetation is often prescribed burned with live moisture content of 60–75%; and drier chaparral burns more violently (Countryman, 1974; Green, 1981). As reported by Sun

[1]The use of trade names is presented for informational purposes only and does not constitute endorsement by the U.S. Department of Agriculture.

Table 1 Skeletal reaction mechanism for pyrolysis gas combustion

No.	Reaction	A	B	E_a
1	$H+O_2=OH+O$	5.13E + 16	−0.82	16507
2	$O+H_2=OH+H$	1.80E + 10	1.00	8826
3	$OH+H_2=H_2O+H$	1.17E + 09	1.30	3626
4	$2OH=O+H_2O$	6.00E + 08	1.30	0
5	$H+O_2+M\Rightarrow HO_2+M$	3.61E + 17	−0.72	0
6	$H+HO_2\Rightarrow 2OH$	1.40E + 14	0.00	1073
7	$H+HO_2\Rightarrow H_2+O_2$	1.25E + 13	0.00	0
8	$OH+HO_2\Rightarrow H_2O+O_2$	7.50E + 12	0.00	0
9	$H+OH+M\Rightarrow H_2O+M$	1.60E + 22	−2.00	0
10	$CO+OH=CO_2+H$	1.51E + 07	1.30	−758
11	$CH_4+H\Rightarrow CH_3+H_2$	2.20E + 04	3.00	8750
12	$CH_4+O\Rightarrow CH_3+OH$	1.60E + 06	2.36	7400
13	$CH_4+OH\Rightarrow CH_3+H_2O$	1.60E + 06	2.10	2460
14	$CH_3+O\Rightarrow CH_2O+H$	6.80E + 13	0.00	0
15	$CH_3+OH\Rightarrow CH_2O+H_2$	1.00E + 12	0.00	0
16	$CH_3+H+M\Rightarrow CH_4+M$	8.00E + 26	−3.00	0
17	$CH_2O+H\Rightarrow HCO+H_2$	2.19E + 08	1.77	3000
18	$CH_2O+OH\Rightarrow HCO+H_2O$	3.43E + 09	1.18	−447
19	$HCO+H\Rightarrow CO+H_2$	4.00E + 13	0.00	0
20	$HCO+OH\Rightarrow CO+H_2O$	5.00E + 12	0.00	0
21	$HCO+O_2\Rightarrow HO_2+CO$	3.30E + 13	−0.40	0
22	$HCO+M\Rightarrow H+CO+M$	1.60E + 14	0.00	14700

Note: Skeletal mechanism is by Zhou and Mahalingam (2001) with updated values of parameters available in most recent version of CHEMKIN-Pro.

M is used in the above reactions as a placeholder for multiple chemical species (CHEMKIN-Pro, 2008).

et al. (2006), it is generally accepted that when the fuel moisture content is below a threshold of 30%, the fuel may be considered essentially dead. Typical dead fuel moisture content may range from 4–5% to nearly 30%. In the present study, the mole fraction X_{H_2O} ranged from 0.01 to 0.65 with increments of 0.1. It is not possible to link the mole fraction of water to a specific live fuel moisture content as the movement and release of water from vegetation due to heating is a complex process that has not be adequately described (Cohen et al., 1990; Fletcher et al., 2007; Jolly et al., 2012).

Laminar Premixed Flame

A laminar premixed flame, which is a one-dimensional configuration with uniform inlet conditions where the oxidizer is mixed with the fuel before reaching the flame front, was simulated using the PREMIX code of CHEMKIN-Pro. This

Table 2 Mole fractions of four gases released during pyrolysis of three different woods

	X_{H2}	X_{CO}	X_{CH4}	X_{CO2}
A (aspen)	0.410	0.256	0.077	0.257
B (beech)	0.253	0.307	0.112	0.328
C (larch)	0.398	0.264	0.112	0.226

code is able to describe the flame dynamics by solving the differential governing equations using the implicit finite differencing method along with a combination of steady state and time dependent methods. The initial temperature and pressure were set to 298 K and 1 atm, respectively. The computational domain size is 13 cm bounded at two points located at − 5 to 8 cm. The flame front is anchored around 1.42 cm.

The fuel compositions used in the premixed flame studied here were the same used in the diffusion flame described in the previous subsection, which are listed in Table 2. The fuel was premixed with air as an oxidizer. The equivalence ratio was set to unity for the initial runs, which were used to measure the composition of the different gas species and temperature with respect to moisture. The moisture content of the fuel was varied similar to that is done in the opposed diffusion flame described in the previous subsection. For instance, when 10% of H_2O is added to the fuel, then the other components of the fuel are multiplied by 0.9 for consistent mole fractions.

RESULTS

Opposed Diffusion Flame

The spatial distribution of temperature within the opposed diffusion flame is plotted in Figure 1 for various water mole fractions. The results were obtained with an adiabatic assumption, i.e., nonradiation heat transfer. For all three types of fuel displayed in Figures 1a–1c, it was observed that at $X_{H_2O} = 0.65$, the temperature curve is flat, indicating that the flame is not sustained at this mole fraction. This observation implies that at a water mole fraction between $X_{H_2O} = 0.60$ and 0.65, the flame is extinguished. Also, it is seen that in the case of aspen and larch shown in Figures 1a and 1c, respectively, there is a significant drop in temperature as X_{H_2O} increases from 0.55 to 0.60, with the flame extinguishing at X_{H_2O} of 0.65, whereas in the case of beech, extinction occurs at X_{H_2O} of 0.60 as can be seen in Figure 1b. For the aspen mixture, as the moisture content increases from 0 to 0.60, the flame temperature drops from 1800 K to 298 K.

Variations of mole fractions of multiple major chemical components including CH_4, CO_2, CO, H_2, H, O_2, and H_2O have been examined in detail. A significant change in the mole fractions of O_2 and H is observed between X_{H_2O} of 0.55 and 0.65. It is seen that O_2 and H are the only components that show significant changes. In the mechanism for hydrogen combustion the oxygen and hydrogen atoms form intermediate species HO_2, which is the hydroperoxy radical, and hydrogen atom, H, as another radical. Here, O_2 and H_2 only require one bond to be broken and one to be formed to form aforementioned intermediate species. These radicals, which are called free radicals, are highly reactive atoms that have either a positive or negative charge, which could then react with other reactions to create more radicals. Therefore, these free radicals become the driving force of the reaction mechanism. Since the hydrogen atom H is one of the most reactive radicals, it is important to look at how the increase in moisture affects H (Turns, 2012). It is noted that in the skeletal reaction mechanism, presented in Table 1, H_2O appears as a reactant in the reversible reaction 3, so it can be said that this reaction represents an input point for the action of water vapor upon the global combustion process.

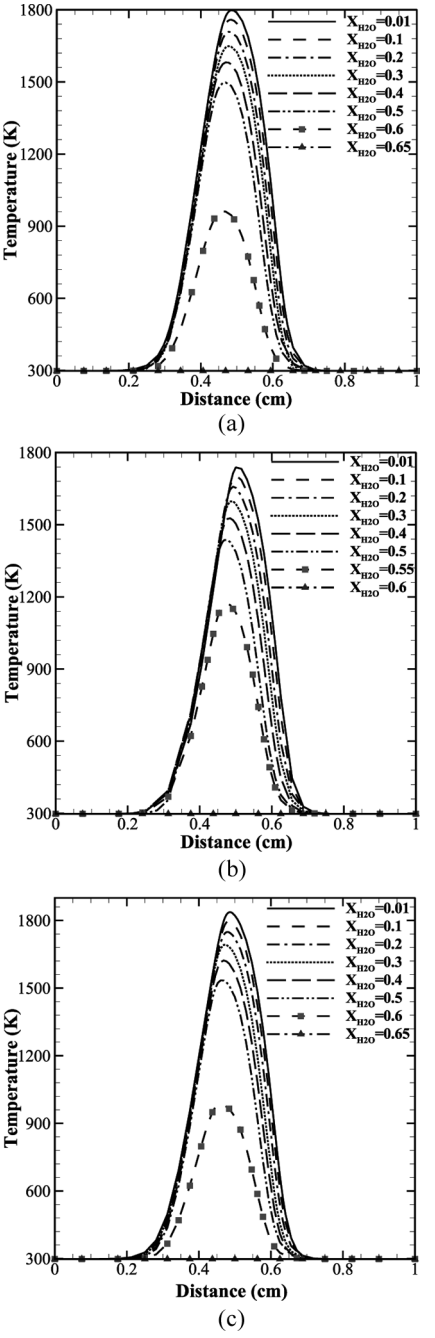

Figure 1 Temperature in the opposed diffusion flame of gas mixtures representing (a) aspen, (b) beech, and (c) larch pyrolyzates.

The mole fraction of O_2 is shown for the range of moisture mole fraction in Figure 2 for the opposed diffusion flame. O_2 is an initial component in the oxidizer stream, which enters from the right boundary. For $X_{H_2O} = 0$, the O_2 mole fraction starts to decline at a distance of 0.7 cm and is fully consumed at an approximate distance of 0.45 cm from the fuel nozzle. As the mole fraction of H_2O increases, the start point of decline of O_2 mole fraction shifts towards the fuel nozzle side. This shift along with a slight shift in maximum temperature visible in Figure 1, shows that the flame is shifting toward the fuel side with a reduction in the total width of the flame.

Figure 3 shows the mole fraction of H in the opposed diffusion flame. The radical H is not an initial component in the fuel or oxidizer streams; however, it is derived from H_2, which is an initial component in the fuel stream. For all three gas mixtures, the mole fraction of H was negligible throughout the domain for $X_{H_2O} \geq 0.65$. Furthermore, a significant decline in H was observed in the range $0.55 < X_{H_2O} < 0.65$. In the case of pyrolysis gases from beech wood, seen Figure 3b, at X_{H_2O} of 0.60, the H mole fraction was nearly zero, and for the cases of aspen and larch (see Figures 3a and 3c), the mole fraction of $H \rightarrow 0$ for $0.6 \leq X_{H_2O} \leq 0.65$, but it was still produced. Also, a slight shift toward the origin is observed for the peak of the mole fraction of H in Figre 3 as X_{H_2O} is increased. This observation is consistent with a similar shift for the peak of temperature (see Figure 1) where the flame is located. Ideally the flame is where the equivalence ratio is stoichiometric.

The maximum flame temperature was calculated for various strain rates in order to determine an extinction strain rate point for aspen wood for various water mole fractions. The strain rate was calculated in the present work following the formulation given for the global strain rate $\dot{\varepsilon} = \left(U_f - U_{ox}\right)/d$ in CHEMKIN-Pro, where U_f is the velocity of the fuel, U_{ox} is the velocity of the oxidizer, and d is the separation distance. The global strain rate was plotted against the maximum temperature in Figure 4. The maximum flame temperature was highest for $X_{H_2O} = 0$ and the extinction point was found to be near $2000 s^{-1}$. As X_{H_2O} was increased, the strain rate extinction point decreased. At $X_{H_2O} = 0.6$, the extinction point of the strain rate was approximately $380\,s^{-1}$. An increase in X_{H_2O} was seen to not only lower the maximum temperature by greater than 400 K, but it was also seen to decrease the extinction point by $1610\,s^{-1}$.

A sensitivity analysis for the diffusion flame is performed in order to identify the chemical reactions that are responsible for the change in temperature when moisture is increased. The sensitivity of temperature to the Arrhenius pre-exponential factor, i.e., A in Eq. (1), of the various reaction-rate constants was investigated. In Table 3, the reactions that are found to be more influential on temperature are listed. The normalized sensitivity coefficient against distance is displayed in Figure 5 for five reactions to which temperature is most sensitive. Among all reactions, the three-body reaction no. 5, $H+O_2+M=HO_2+M$, had both the most positive and negative sensitivity coefficient values.

Laminar Premixed Flame

No ignition occurred for the laminar premixed flame when X_{H_2O} was larger than 0.7 for aspen and larch fuel or larger than 0.65 for beech fuel (Figures 6a, 6c, and 6b, respectively). As H_2O mole fraction was increased, the flame thickness

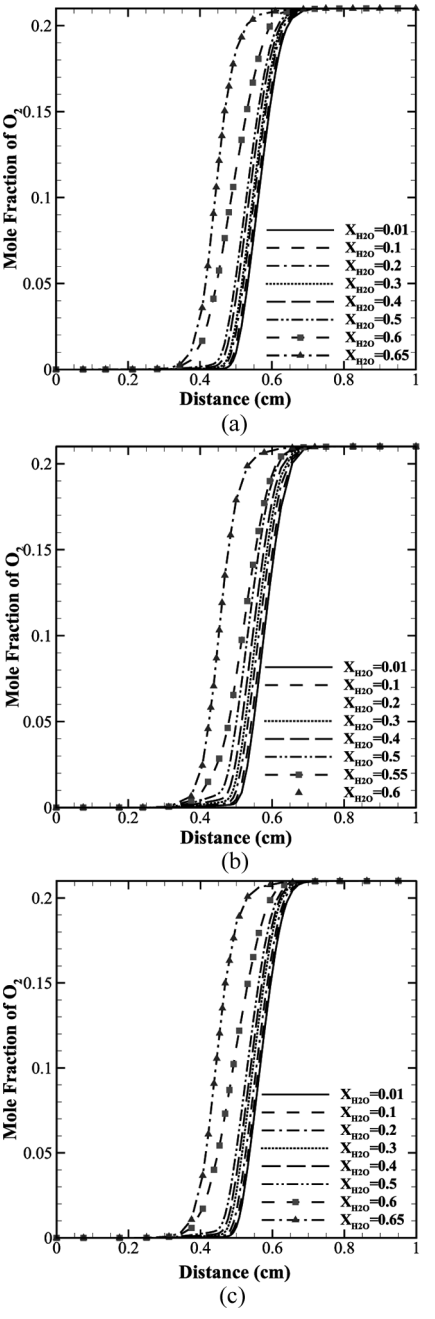

Figure 2 Mole fraction of O_2 in the opposed diffusion flame of gas mixtures representing (a) aspen, (b) beech, and (c) larch pyrolyzates.

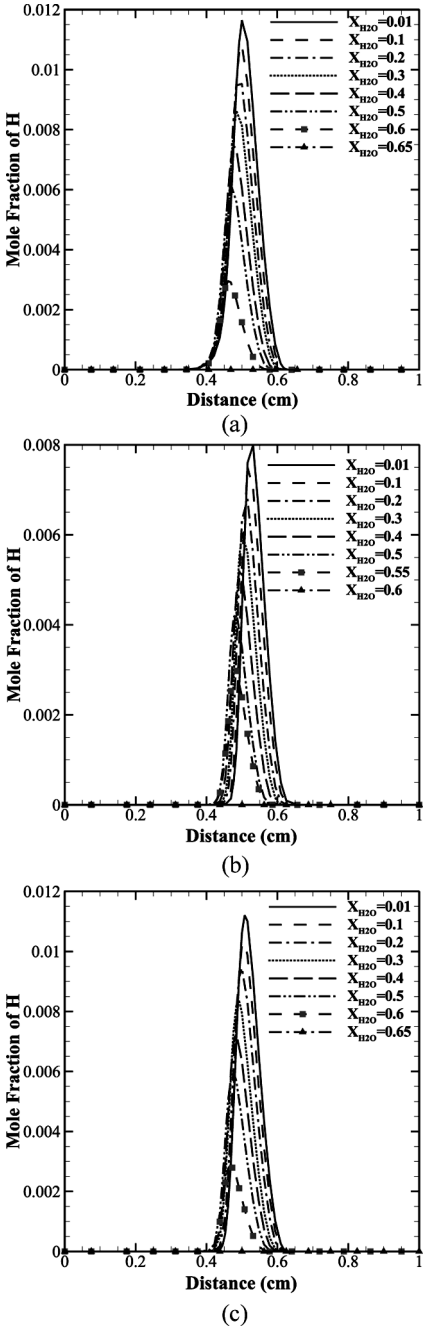

Figure 3 Mole fraction of H in the opposed diffusion flame of gas mixtures representing (a) aspen, (b) beech, and (c) larch pyrolyzates.

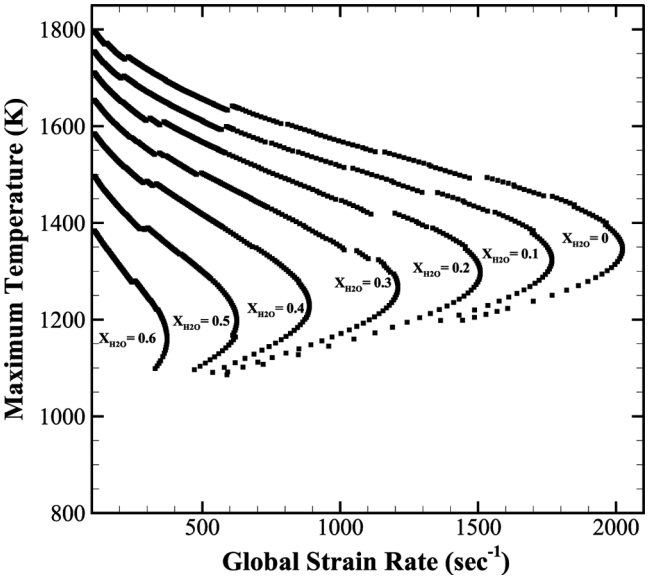

Figure 4 Global strain rate versus maximum temperature in the opposed diffusion flame for various mole fractions of H_2O in the pyrolyzate mixture produced from aspen wood. The flame exits at a maximum temperature of 1200 K.

increased, as determined by the slope at which the temperature rises (Turns, 2012), while the burned gas temperature decreases. This behavior is attributed to the fall of the energy release rate, as will be seen later in this section, with the rise of X_{H_2O}.

The spatial variations of the mole fractions of H and O_2 are shown in Figures 7 and 8, respectively. The species composition of the hydrogen radical shows that H is not made for X_{H_2O} greater than 0.7 in the case of aspen and larch fuel (see Figures 7a and 8b) and greater than 0.65 for beech fuel in Figure 7b. Since the flame does not ignite at those temperatures, it can be inferred that the reaction process that

Table 3 Reactions associated with temperature sensitivity to the Arrhenius A-factor (The number for the reaction is from Table 1)

No.	Reaction
1.	$H + O_2 = OH + O$
3.	$OH + H_2 = H_2O + H$
5.	$H+O_2+M \Rightarrow HO_2+M$
6.	$H+HO_2 \Rightarrow 2OH$
9.	$H+OH+M \Rightarrow H_2O+M$
11.	$CH_4+H \Rightarrow CH_3+H_2$
10.	$CO + OH = CO_2 + H$
14.	$CH_3+O \Rightarrow CH_2O+H$
15.	$CH_3+OH \Rightarrow CH_2O+H_2$
16.	$CH_3+H+M \Rightarrow CH_4+M$
19.	$HCO+H \Rightarrow CO+H_2$
22.	$HCO+M \Rightarrow H+CO+M$

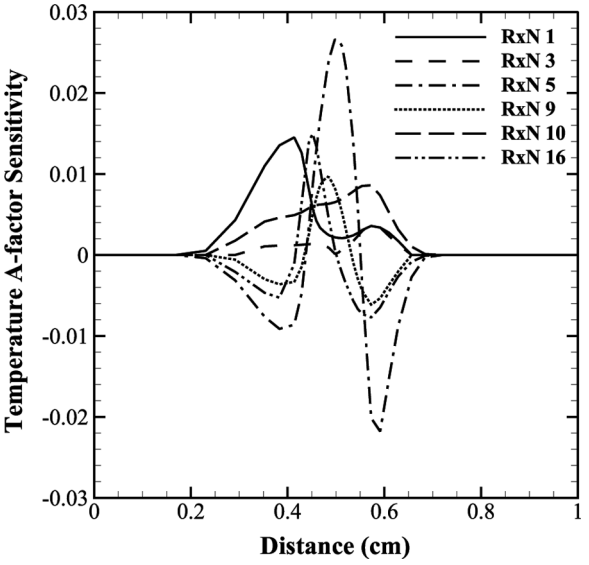

Figure 5 Effect of distance from the fuel nozzle on the temperature Arrhenius A-factor to various reactions for an H_2O mole fraction of 0.5 for a gas mixture representing pyrolyzates from aspen wood.

produces the H radical did not occur. At lower X_{H_2O}, the slopes of the X_{O_2} curves were greater than those at higher X_{H_2O}, which indicates that that less O_2 was used in the reaction process.

Figure 9 shows the net energy release rate in the considered premixed flame. The importance of this parameter in fire has been discussed by Babrauskas and Peacock (1992) and Van Wagner (1976). The energy release rate in the flame typically increased rapidly from the point of flame attachment, reached a maximum, decreased rapidly, and then became nearly constant (Figure 9). The plateau seen in Figure 9 is due to the radical bond dissociation energy (Turns, 2012) and is most impacted by reactions 3, 9, and 10, listed in Table 1, since they are the only reactions that display a significant plateau or decrease in the energy release rate. For all fuel types, the energy release rate decreases as the moisture content increases. Therefore, the intensity of the fire decreases as the moisture rate increases. As a result, it is expected that the propagation time will be slower, the ability to initiate new fires will decrease, and the ability to sustain a flame will decrease for higher moisture contents. The energy release rate is not plotted for X_{H_2O} greater than 0.7 for aspen and larch fuel mixtures and for X_{H_2O} greater than 0.65 for beech fuel, since no energy is released or absorbed because the flame is not ignited at those moisture contents. Reactions 1, 3, 4, 5, 6, 9, 10, 14, 16, 17, and 19 from Table 1 had the most significant effect on the net energy release rate, since a significant amount of energy released is seen for each individual previously mentioned reaction. For highly branched reactions, only the reaction with recombination of active centers will lead to heat release (Korobeinichev and Bolshova, 2011). Heat release occurs during the recombination of hydrogen atoms. For example, reaction 2 from Table 1 shows the breaking bond of H and no recombination of the two H atoms; therefore, no heat release is

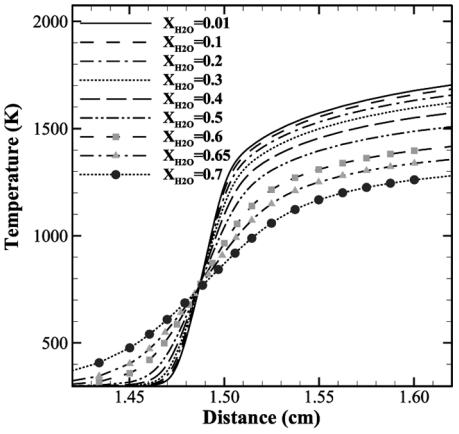

(a)

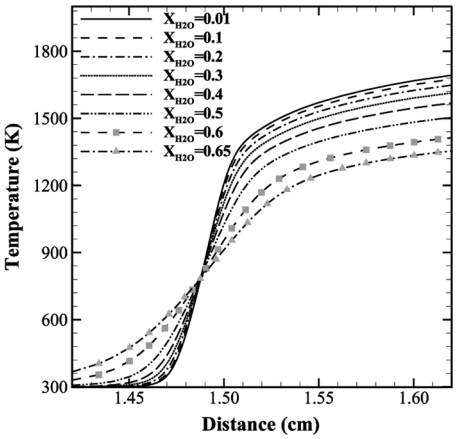

(b)

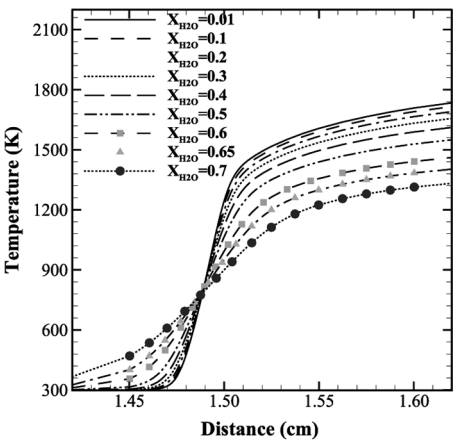

(c)

Figure 6 Effect of distance from the flame anchor point (flame front) on temperature in a premixed flame for mixtures of gases representing pyrolyzates from (a) aspen, (b) beech, and (c) larch wood.

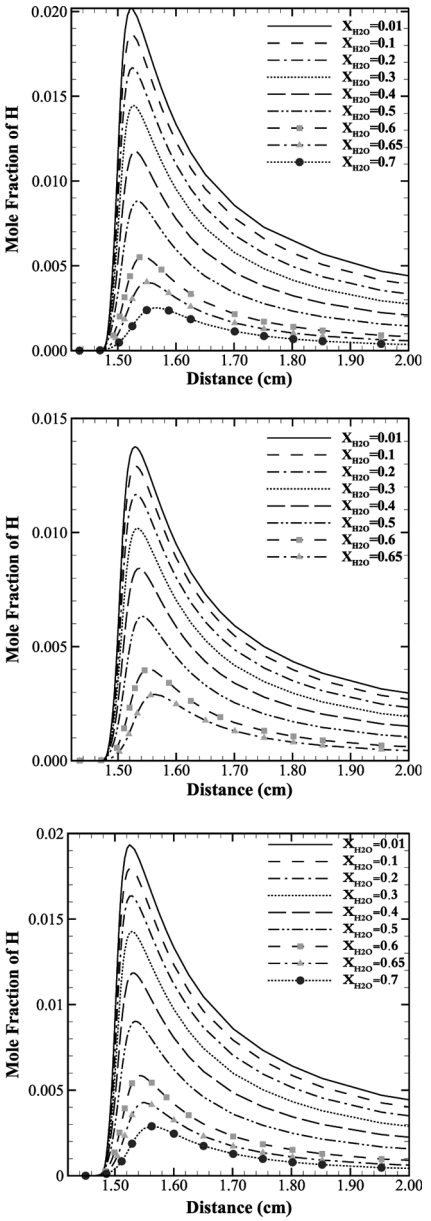

Figure 7 Mole fraction of H in the laminar premixed flame of gas mixtures representing (a) aspen, (b) beech, and (c) larch pyrolyzates.

observed in that reaction. In other reactions, the amount of energy required to break a bond may be equal or greater than the amount of energy required to create a new bond. In the cases where the energy required to break a bond is equal or nearly equal to the amount required to form a new bond, the net energy release rate for the reaction would be near zero. The reaction that has the highest maximum energy release

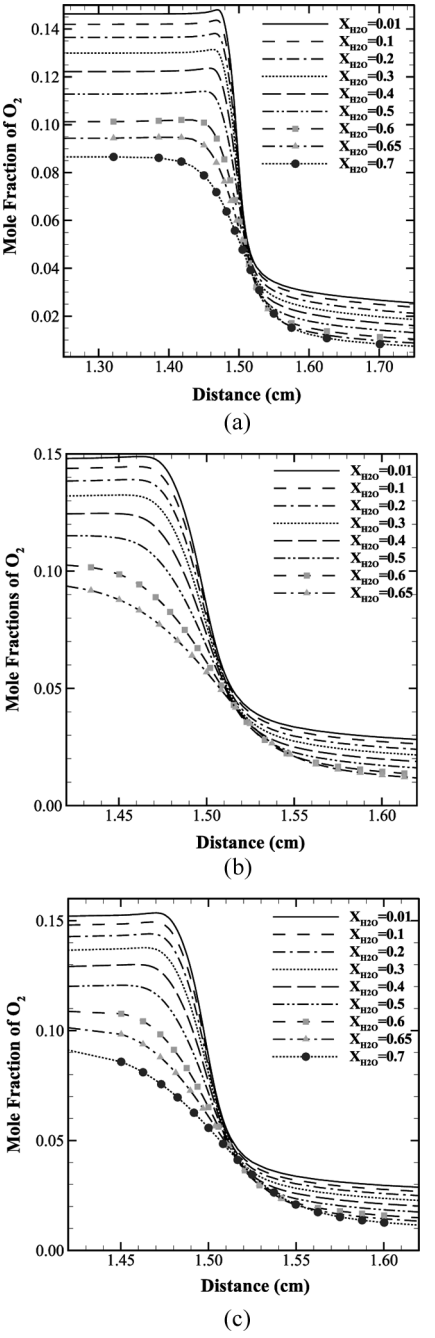

Figure 8 Mole fraction of O_2 in the laminar premixed flame of gas mixtures representing (a) aspen, (b) beech, and (c) larch pyrolyzates.

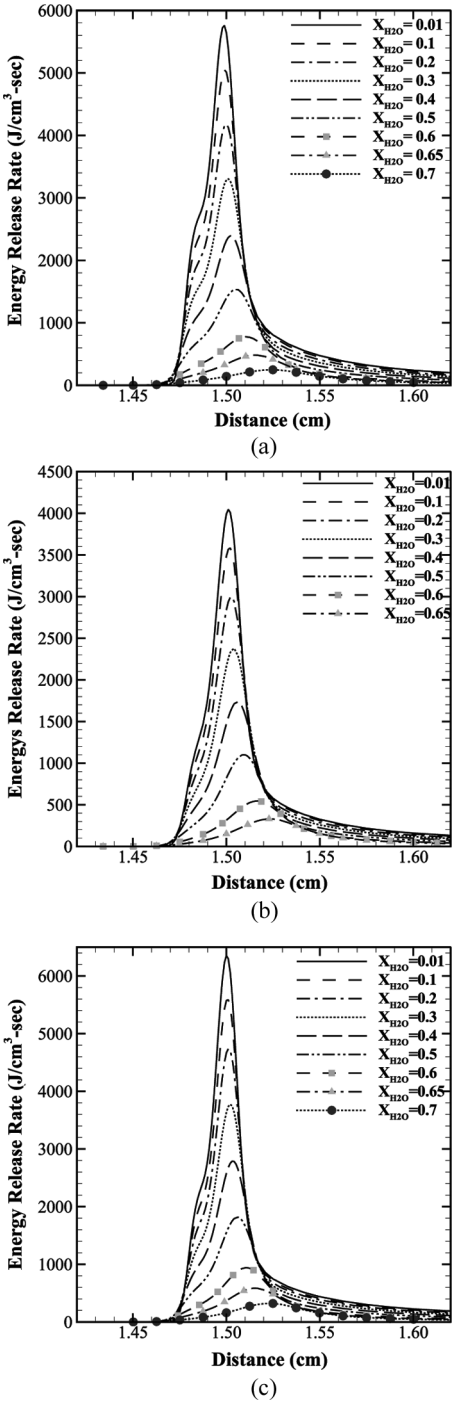

Figure 9 Net energy release rate in the laminar premixed flame of gas mixtures representing (a) aspen, (b) beech, and (c) larch pyrolyzates.

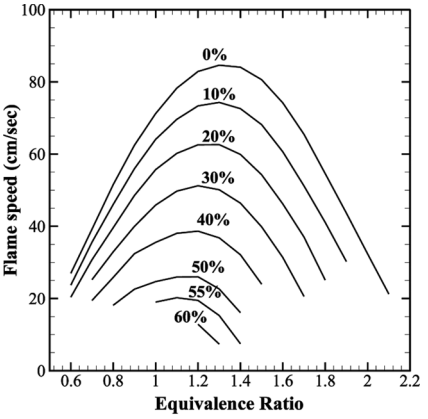

(a)

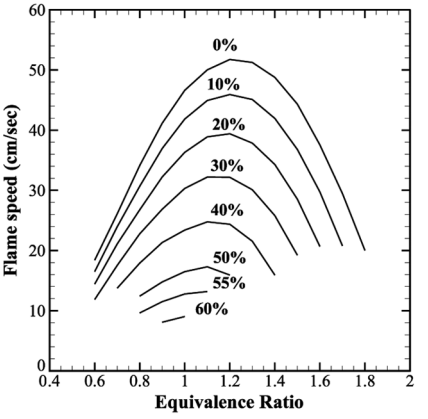

(b)

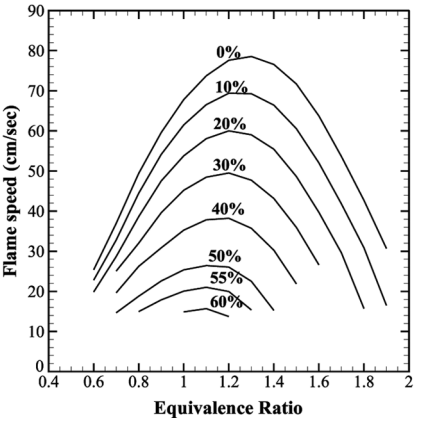

(c)

Figure 10 The effect of the equivalence ratio on flame speed in the laminar premixed flame of a gas mixture: (a) aspen, (b) beech, and (c) larch pyrolyzate.

rate is reaction 14 from Table 1 with a maximum energy release rate of $1800\,J/cm^3$-sec. Reactions 3, 16, and 19 have the next greatest impact on the net energy release rate with maximum individual energy release rates over $1000\,J/cm^3$-sec.

The flame speed is typically used to characterize the combustion of various fuel-oxidizer combinations. It is also useful in determining the flammability limits of mixtures. The flame speed was simulated using CHEMKIN-Pro for all three fuel types and plotted against different equivalence ratios in Figure 10 for various moisture contents. As the moisture content increased, not only did the flame speed decrease, but the ability of the flame to sustain in a fuel rich or lean environment also decreases. The flame is seen to only ignite under ideal fuel/oxidizer ratios. Since the fuel and air ratios cannot be controlled in natural environment, it is expected that the flame will not ignite in the field experiments for higher moisture rates, even though it can be seen in experiments and simulations where the fuel/air ratio is controlled. For the lowest considered moisture content, which is 60%, the flame ignites only for a few equivalence ratios. It is observed that the flame only thrives in slightly fuel-rich conditions for aspen and larch at 60% moisture content and in slightly fuel-lean to ideal conditions for beech. The maximum flame speed, for all types of fuel mixtures, seemed to take place for equivalence ratios in a domain ranging from 1.1 to 1.3. The maximum flame speed is shifted toward higher equivalence ratio areas with the increase of the moisture content.

SUMMARY AND CONCLUSIONS

Wildland fires often burn live vegetation that holds a significant amount of moisture, which is released to the gaseous phase as the cellulose and hemicellulose in the vegetation are pyrolyzed. Ignition of pyrolysis gases produces a gaseous flame, which is important to model in order to characterize the behavior of the fire. By characterizing the gaseous fire that includes the moisture found in live vegetation, a more accurate mechanism can be developed to better understand the fire's behavior.

The water vapor, which originates from the moisture content in vegetation, was found to have an impact on the temperature distribution within both an opposed diffusion flame and a premixed laminar flame for three types of fuels. For the opposed diffusion flame, the temperature steadily decreased as the moisture content was increased until a significant decrease was observed at mole fraction $X_{H_2O} = 0.55$. Between $X_{H_2O} = 0.55$ and 0.65, the flame extinguished for all the cases we examined. For the premixed laminar flame, the slope of temperature decreases, meaning the flame front increased as the moisture content increased. The flame was extinguished between $X_{H_2O} = 0.65$ and 0.7 for all cases.

In order to understand the role of chemistry on flame extinction, the distribution of major gas components was examined. The components that showed dramatic changes were O_2 and H for both the non-premixed and premixed flame. The influence of the strain rate on the non-premixed flame was investigated as the maximum temperature was obtained for various strain rates. It was determined that moisture content of 0.1 preserved the flame at the highest strain rate of $350\,s^{-1}$. The sensitivity analysis was also performed in the opposed diffusion flame to identify reactions that could potentially contribute to the observed reduction in flame temperature and its eventual extinction. In the premixed flame, both the laminar flame speed and

the energy release rate were examined in the premixed flame for various water mole fractions. The energy release rate showed that the intensity of the flame decreased as the moisture content increased. In the laminar premixed flame, the flame speed model showed that at a higher moisture content of 60%, the flame existed at a slightly fuel-rich equivalent ratio for aspen and larch, and a slightly fuel-lean equivalent ratio for beech. For the premixed flame, the length of the flame front increased and the temperature decreased as the moisture rate decreased. In all cases the flame was extinguished or failed to ignite with moisture content greater than 70%.

In the future, we will further investigate whether the reactions that were found to play a significant role in affecting the flame in this article should be included in a reduced mechanism for use in wildland fire behavior models. A new reduced mechanism will be developed based on reactions that show significant importance to the effect of moisture. Our ultimate goal is to develop a new reduced mechanism that takes into consideration live vegetation that is burned in wildland fires and compare it to that reported in Zhou and Mahalingam (2001).

ACKNOWLEDGMENT

The authors gratefully acknowledge financial support from the USDA Forest Service PSW Research Station through cooperative agreement 10-JV-11272166-091 awarded to the University of Alabama in Huntsville.

REFERENCES

Albini, F.A. 1981. A model for the wind-blown flame from a line fire. *Combust. Flame*, **43**, 155–174.

Anderson, H.E. 1969. Heat transfer and fire spread. USDA Forest Service Research Paper INT-69, Intermountain Forest and Range Experiment Station, Ogden, UT.

Babrauskas, V., and Peacock, R. 1992. Heat release rate: The single most important variable in the fire hazard. *Fire Saf. J.*, **18**, 255–272.

Beringer, J., Hutley, L., Tapper, N., Coutts, A., Kerley, A., and Grady, A. 2003. Fire impacts on surface heat, moisture and carbon fluxes from a tropical savanna in northern Australia. *Int. J. Wildland Fire*, **12**, 333–340.

Bryden, K.M., and Hagge, M.J. 2003. Modeling the combined impact of moisture and char shrinkage on the pyrolysis of a biomass particle. *Fuel*, **82**, 1633–1644.

Bryden, K.M., Ragland, K., and Rutland, C. 2002. Modeling thermally thick pyrolysis of wood. *Biomass Bioenergy*, **22**, 41–53.

CHEMKIN-PRO. 2008. Reaction Design, San Diego.

Cohen, W.B., Omi, P.N., and Kaufmann, M.R. 1990. Heating-related water transport to intact lodgepole pine branches. *For. Sci.*, **36**, 254.

Countryman, C.M. 1974. Moisture in living fuels affects fire behavior. *Fire Management Notes*, **35**(2), 10–14.

Fletcher, T.H., Pickett, B.M., Smith, S.G., Spittle, G.S., Woodhouse, M.M., Haake, E., and Weise, D.R. 2007. Effects of moisture on ignition behavior of moist California chaparral and Utah leaves. *Combust. Sci. Technol.*, **179**, 1183–1203.

Green, L.R. 1981. Burning by prescription in chaparral. General Technical Report PSW-51. U.S. Department of Agriculture, Forest Service, Pacific Southwest Forest and Range Experiment Station, Albany, CA. http://treesearch.fs.fed.us/pubs/24106

Jolly, W.M., Parsons, R.A., Hadlow, A.M., Cohn, G.M., McAllister, S.S., Popp, J.B., Hubbard, R.M., and Negron, J.F. 2012. Relationships between moisture, chemistry, and ignition of *Pinus contorta* needles during the early stages of mountain pine beetle attack. *For. Ecol. Manage.*, **269**, 52–59.

Klose, W., Damm, S., and Wiest, W. 2000. Pyrolysis and Activation of different woods-thermal analysis (TG/EGA) and formal kinetics. In *Proceedings of the 4th International Symposium on Cataytic and Thermochemical Conversion of Natural Organic Polymers*, May 30–June 3, Krasnoyarsk, Russia, pp. 9–17.

Korobeinichev, O.P., and Bolshova, T.A. 2011. Increasing the burning velocity of a low-pressure hydrogen-oxygen flame by the addition of trimethyl phosphate in terms of Zel'dovich's chain mechanism of flame propagation. *Combust. Explos. Shock Waves*, **47**, 12–18.

Lee, D.H., Yang, H., Yan, R., and Liang, D.T. 2007. Prediction of gaseous products from biomass pyrolysis through combined kinetic and thermodynamic simulations. *Fuel*, **87**, 410–417.

Leroy, V., Leoni, E., and Santoni, P. 2008. Reduced mechanism for the combustion of involved gases in forest fires. *Combust. Flame*, **154**, 410–433.

Lutz, A.E., Kee, R.J., Grcar, J.F., and Rupley, F.M. 1997. OPPDIF: A Fortran program for computing opposed-flow diffusion flames. Sandia National Laboratories Report SAND96–8243. Office of Scientific and Technical Information, OSTI, U.S. Department of Energy.

Manzello, S.L., Maranghides, A., and Mell, W.E. 2007. Firebrand generation from burning vegetation. *Int. J. Wildland Fire*, **16**, 458–462.

McDonald, J., Zielinska, B., Fujita, E., Sagebiel, J., Chow, J., and Watson, J. 2000. Fine particles and gaseous emission rates from residential wood combustion. *Environ. Sci. Technol.*, **34**, 2080–2091.

Morvan, D., and Dupuy, J.L. 2004. Modeling the propagation of a wildfire through a Mediterranean shrub using a multiphase formulation. *Combust. Flame*, **138**, 199–210.

Smith, G.P., Golden, D.M., Frenklach, M., Moriarty, N.W., Eiteneer, B., Goldenberg, M., Bowman, C.T., Hanson, R.K., Song, S., Gardiner, W.C.Jr., Lissianski, V.V., and Qin, Z. 2000. GRI-Mech. http://www.me.berkeley.edu/gri_mech/

Som, S., Ramirez, A.I., Hagerdorn, J., Saveliev, A., and Aggarwal, S.K. 2008. A numerical and experimental study of counterflow syngas at different pressures. *Fuel*, **87**, 319–334.

Sun, L., Zhou, X., Mahalingam, S., and Weise, D.R. 2006. Comparison of burning characteristics of live and dead chaparral fuels. *Combust. Flame*, **144**, 349–359.

Tihay, V., and Gillard, P. 2010. Pyrolysis gases released during the thermal decomposition of three Mediterranean species. *J. Anal. Appl. Pyrolysis*, **88**, 168–174.

Turns, S.R. 2012. *An Introduction to Combustion: Concepts and Applications*, 3rd ed., McGraw-Hill, New York.

Van Wagner, C. 1976. Conditions for the start and spread of crown fire. *Can. J. For. Res.*, **7**, 23–34.

Williams, R.J., Gill, A.M., and Moore, P.H.R. 1998. Seasonal changes in fire behaviour in a tropical savanna in northern Australia. *Int. J. Wildland Fire*, **8**, 227–239.

Zhou, X., and Mahalingam, S. 2001. Evaluation of reduced mechanism for modeling combustion of pyrolysis gas in wildland fires. *Combust. Sci. Technol.*, **171**, 39–70.

Zhou, X., Mahalingam, S., and Weise, D. 2005a. Modeling of marginal burning state of fire spread in live chaparral shrub fuel bed. *Combust. Flame*, **143**, 183–198.

Zhou, X., Weise, D., and Mahalingam, S. 2005b. Experimental measurements and numerical modeling of marginal burning in live chaparral fuel beds. *Proc. Combust. Inst.*, **30**, 2287–2294.